

Sensitivity of predicted liquefaction-induced lateral spreading displacements from the 2010 Darfield and 2011 Christchurch earthquakes

K Robinson, M Cubrinovski, B A Bradley

Department of Civil and Natural Resource Engineering, University of Canterbury, Christchurch
kelly.robinson@pg.canterbury.ac.nz (Corresponding author)

Keywords: liquefaction, lateral spreading, Canterbury Earthquakes

ABSTRACT

The 2010 Darfield and 2011 Christchurch Earthquakes triggered extensive liquefaction-induced lateral spreading proximate to streams and rivers in the Christchurch area, causing significant damage to structures and lifelines. A case study in central Christchurch is presented and compares field observations with predicted displacements from the widely adopted empirical model of Youd et al. (2002). Cone penetration testing (CPT), with measured soil gradation indices (fines content and median grain size) on typical fluvial deposits along the Avon River were used to determine the required geotechnical parameters for the model input. The method presented attempts to enable the adoption of the extensive post-quake CPT test records in place of the lower quality and less available Standard Penetration Test (SPT) data required by the original Youd model. The results indicate some agreement between the Youd model predictions and the field observations, while the majority of computed displacements error on the side of over-prediction by more than a factor of two. A sensitivity analysis was performed with respect to the uncertainties used as model input, illustrating the model's high sensitivity to the input parameters, with median grain size and fines content among the most influential, and suggesting that the use of CPT data to quantify these parameters may lead to variable results.

1 INTRODUCTION

The Darfield Earthquake of 4 September 2010 (M_w 7.1) and the Christchurch Earthquake of 22 February 2011 (M_w 6.2) triggered extensive liquefaction throughout Christchurch and surrounding suburbs. In particular, liquefaction-induced horizontal ground displacements ('lateral spreading') resulted in severe damage to structures and lifelines in proximity to streams and rivers (Cubrinovski et al. 2012). There is a clear need to understand and predict the extent of lateral spreading movements and the consequent hazard to buildings and infrastructure under future earthquake scenarios. However, the uncertainty in the prediction of lateral spreading is compounded by the large uncertainty in ground motion estimation and variability in site conditions.

Case histories of lateral spreading occurrence during historic earthquakes have been collated and used to develop simple empirical and semi-empirical models for estimating the magnitudes of lateral displacement (e.g. Youd et al. 2002, Zhang et al. 2004). With uncertainties in spreading displacement estimates often on the order of +/-50% (i.e. a factor of two), the predictions are suitable for characterising the hazard within an order of magnitude, but are often inadequate for detailed design.

This paper compares field measurements of lateral spreading displacements obtained following the Christchurch earthquake with displacement predictions using the Youd et al. (2002) model. Cone penetration test (CPT) data was used to classify the geotechnical input parameters for the model, as Standard Penetration Test (SPT) data in proximity to the field measurements was scarce or unavailable. Abundant CPT and grain size data (fines content, FC , and median grain size, D_{50}) along the Avon River were used to develop site-specific correlations for estimating the F_{15} and $D_{50(15)}$ parameters, where these are defined below. The associated uncertainties with

these relationships, as well as with the remaining input values used in the comparison, are addressed in a sensitivity analysis for a specific location.

2 YOU D ET AL. (2002) MODEL

You d et al. (2002) employed regression analysis on documented field measurements of lateral spreading following earthquakes in the US and Japan. Regression parameters considered were related to the ground motion (via. earthquake magnitude and distance parameters), topography (i.e. free face or sloping ground cases), and geotechnical properties (thickness of potential liquefied sliding mass and intrinsic soil gradation characteristics). The functional form of the equation developed for free-face conditions is given in Equation (1) and will hereafter be referred to as the You d et al. model.

$$\log D_H = -16.713 + 1.532M_w - 1.406\log R^* - 0.012R + 0.592\log W + 0.540\log T_{15} + 3.413\log(100 - F_{15}) - 0.795\log(D_{50(15)} + 0.1\text{mm}) \quad (1)$$

where D_H is the lateral spreading displacement (m); M_w is the earthquake moment magnitude; R is the horizontal distance to the nearest seismic source or fault rupture (km); $R^*=R+R_0$ is the modified source distance, where $R_0=10^{(0.89M_w-5.64)}$; $W=H/L*100$ is the free-face ratio, where H is the height of free-face and L is the distance from the crest of the free-face; T_{15} is the thickness (m) of saturated, cohesionless sediment with SPT $(N_1)_{60}<15$; F_{15} is the average fines content, FC (%) within T_{15} ; and $D_{50(15)}$ is the median grain size, D_{50} (mm) within T_{15} . The free-face equation is presented (as opposed to that for sloping ground conditions) as it is more applicable for many of the areas investigated in Christchurch where slopes are relatively gentle (generally less than ~1-2%) and the river channel serves as the free-face.

3 CASE STUDY OF LATERAL SPREADING FIELD MEASUREMENTS

3.1 Site Location

The Avon Loop, situated in the north-east of the Central Business District in Christchurch, was subject to significant lateral spreading following the recent seismic events. Within approximately one month following the 22 February Christchurch Earthquake, field measurements in the area were employed following the Christchurch Earthquake using the method of ground surveying which consists of recording crack dimensions and distance from the waterway in a line (transect) oriented perpendicular to the direction of spreading (Robinson et al. 2011, 2012). Summation of the cracks along the specific line of measurement yielded maximum lateral ground displacements at the river bank ranging from <0.1 m to ~1.6 m. Ground surveying data was not performed at this location following the Darfield event, and hence the measurements are assumed to be cumulative for both the Darfield and Christchurch earthquakes. The surveyed transects and nearby CPT locations are shown in Figure 1 where the colour-coded circles (grouped by 20-centimeter categories) indicate magnitude of cumulative lateral spreading displacement at each point of measurement along the transect, i.e. crack location, start or end of transect.

3.2 Collated geotechnical data

Abundant CPT and SPT borehole (BH) data was collated from sites along the Avon River to develop relationships for estimating the required You d et al. model parameters, specifically F_{15} and $D_{50(15)}$ from CPT data (CERA 2012). There is relatively limited borehole (with SPT) data in close proximity (< 50 m) of the majority of surveyed locations (Fig. 1(a)). Of the boreholes shown, many had very little associated D_{50} and FC data needed for the model input. As a result, an attempt has been made to establish correlations for FC and D_{50} from boreholes with SPT, and the soil behaviour type index (I_c) obtained from CPT test results (You d et al. 2001). In principle, this approach is not recommended as I_c , a measure of soil behaviour type, is not a direct means of determining grain size characteristics; however, due to the current scarcity of available soil gradation data at individual sites where lateral spreading occurred, the CPT data serve as the best resource to quantify the F_{15} and $D_{50(15)}$ You d et al. model parameters.

Available data on the Canterbury Geotechnical Database (CERA 2012) for sites: (i) between Hagley Park in central Christchurch; (ii) the Estuary in the east of the city; and (iii) situated within 300 m of the Avon River and Bottle Lake suburb (a legacy meander loop of the Avon River) were considered. The collated data was limited to boreholes with available soil gradation information (fines fraction and/or particle size distribution curve) and located within 5 meters of a CPT, which totalled 61 sites (Fig. 1(b)).

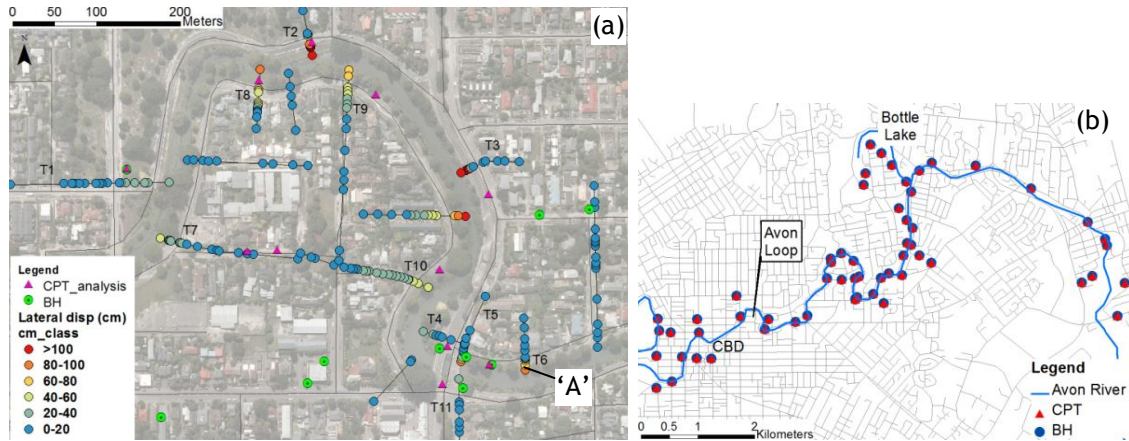


Figure 1. Location plan of (a) cumulative lateral spreading field measurements in the Avon Loop following the Feb 2011 EQ and (b) collated SPT and CPT data for analysis

3.3 Development of geotechnical model parameters, F_{15} and $D_{50(15)}$

3.3.1 Estimation of fines content, FC , from CPT data

A relationship between soil behaviour type index, I_c (after Youd et al. (2001)), and fines content, FC , specific to the soils subject to lateral spreading along the Avon River was developed from the available CPT and nearby boreholes with soil gradation data. A simplified soil profile was developed based on interpretation of CPT tip resistance, q_c , and computed soil behaviour type, I_c , in order to obtain approximate I_c -values at depths corresponding to the soil gradation data in adjacent boreholes. The interpreted strata were compared to the borehole logs to ensure consistency in the soil description for the sample and selected I_c -layer. Figure 2 presents the site-specific relationship developed between I_c and FC . The I_c -value within an interpreted soil layer typically varied on the order of ± 0.1 to ± 0.2 , as represented by the horizontal error bars in the plot. Strata that exhibited significant variation in I_c (typically $> \pm 0.3$), e.g. at a transition zone between two layers, were not included in the analysis.

To develop a parametric relationship between I_c and FC , two distinct zones of data were considered, as delineated by $FC=30\%$. Previous research shows the soil-skeleton behavior of sand transitions from a sand-controlled matrix to that of fines-controlled matrix at a threshold fines content of around 30% (e.g. Cubrinovski et al. 2010). Similarly, the selected zone boundary is consistent with liquefaction resistance curves adjusted for fines up to 35% (e.g. Youd et al. 2001). When compared to the general empirical correlation proposed by Robertson and Wride (1998), the Christchurch data for $FC>30\%$ generally fits with the Robertson and Wride bound for low-plasticity soils ($PI<5\%$), as expected given the non-plastic nature of the fluvial silty sands prevalent in Christchurch. In addition, the $FC>30\%$ data is typically bounded by the soil-type behavior line defined by Robertson and Wride (1998) of $I_c=2.05$. Figure 2 provides a relationship to approximate FC from CPT-derived I_c (for $I_c>2.05$); \pm sigma should be considered when employing this relationship given the relatively large amount of uncertainty ($R^2=0.48$). A larger degree of scatter associated with the $FC<30\%$ data indicates no apparent trend, illustrating a decreasing sensitivity of I_c to soils with lower FC . Due to the lack of I_c - FC correlation for soils with $FC<30\%$, an average fines content of 7% (\pm sigma) has been adopted in the Youd et al. model analyses for $I_c<2.05$.

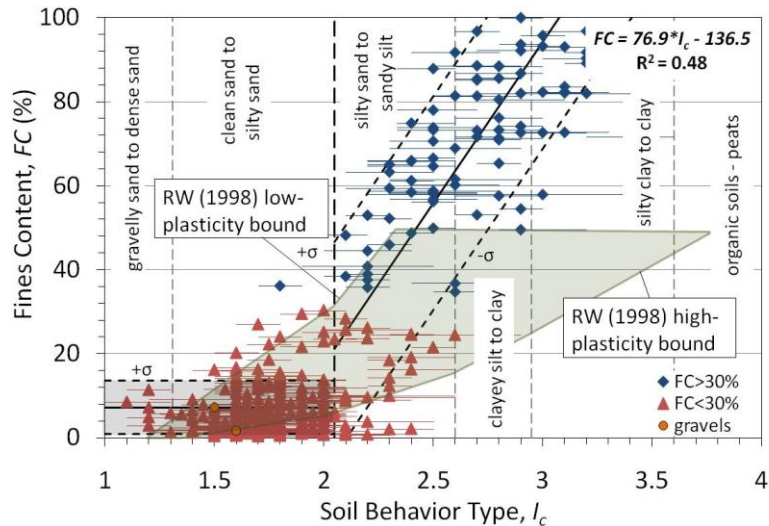


Figure 2. Correlation between FC and I_c for Christchurch soils in comparison to the general relationship of Robertson and Wride (1998)

3.3.2 Estimation of median grain size, D_{50}

To estimate the $D_{50(15)}$ parameter for the Youd et al. model, trends between D_{50} , I_c , and FC were examined using the same data discussed in the last section. Figure 3(a) illustrates the very weak correlation between D_{50} and I_c . However, Figure 3(b) indicates a stronger correlation exists between FC and D_{50} , particularly for soils with $FC > 30\%$. The relationship provided in Figure 3(b) may be used for estimating D_{50} for a given FC (for $FC > 30\%$). In general, for sandy soils with $FC < 30\%$, D_{50} typically ranges between approximately 0.08-0.3mm (+/-sigma) with an average value of about 0.19mm. Thus, the analysis will consider the F_{15} -value from the CPT-based correlations above (Fig. 2) to determine a corresponding $D_{50(15)}$ parameter using the equation in Figure 3(b) for $F_{15} > 30\%$ or an average value of 0.19mm for $F_{15} < 30\%$. The cumulative uncertainty associated with using F_{15} to determine D_{50} is noted and further illustrates that actual grain size data at the site is strongly preferred over these CPT-based relationships. The significance of the variability within these applied correlations is assessed in the subsequent sensitivity analysis.

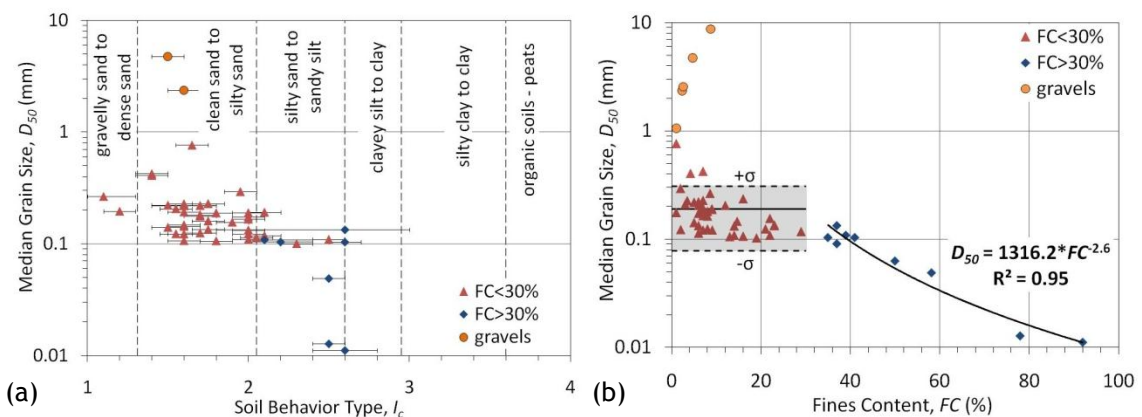


Figure 3. Relationship for Christchurch soils between D_{50} and (a) I_c and (b) FC

4 COMPARISON OF FIELD OBSERVATIONS AND YOUND ET AL MODEL PREDICTIONS

Transects along the Avon Loop located within 50 m of a CPT were considered for the comparison of observed spreading displacements with predictions from the Youd et al model. This included 11 of the 15 surveyed transects shown in Figure 1, labelled as 'T1'-'T11'.

4.1 Determination of input parameters

The parameter T_{15} is defined by Youd et al. (2002) as pertaining to saturated, cohesionless material with corrected, normalised SPT $(N_1)_{60} < 15$. In order to compute T_{15} using CPT data, an equivalent threshold of normalized tip resistance, $q_{c1} < 8 \text{ MPa}$, was used, based on a $q_c(\text{MPa})/N(\text{blows per } 300\text{mm})$ ratio provided by Jeffries and Davies (1993) of about 0.5 for medium sand ($D_{50} \sim 0.2\text{mm}$). To satisfy the “saturated, cohesionless” conditions, material with an $I_c > 2.6$ (indicative of plastic, fine-grained soil response, typically of low susceptibility to liquefaction), or above the groundwater table, were not considered to contribute to T_{15} . This interpretation of T_{15} is consistent with previous comparisons of the Youd et al. (2002) model using CPT data; e.g. Chu et al. (2006).

Using the grain-size relationships described previously, the F_{15} and $D_{50(15)}$ parameters were estimated using the following approach: The equation presented in Figure 2 was used to compute FC for each I_c -value > 2.05 within T_{15} ; for $I_c < 2.05$ within T_{15} , an average value of $FC = 7\%$ was used. These values were then averaged to yield F_{15} . Upper and lower bounds for F_{15} were considered by repeating the calculation with respect to \pm one sigma bound (Fig. 2). The F_{15} -value was then used to determine the appropriate $D_{50(15)}$ value either computed from the equation in Figure 3(b) for $F_{15} > 30\%$, or taken as an average value of 0.19mm for $F_{15} < 30\%$. The uncertainties associated with the D_{50} - FC relationships are recognised and discussed further in the subsequent sensitivity analysis.

Groundwater depths at the time of each event were estimated at the CPT locations using the appropriate groundwater models provided by Tonkin and Taylor for each of the events, 4 September 2010 and 22 February 2011 (CERA 2012). The free-face ratio, W , was computed from the channel height, H , estimated at each location using LiDAR elevation data flown post September 2010 event (CERA 2012), and the distance, L , taken as the distance from the CPT to the waterway. The analysis was limited to $20\% > W > 1\%$, per the Youd et al. model specifications. Site-to-source distance, R , and peak ground acceleration, PGA, values at the site were obtained from Bradley & Hughes (2012). The PGA was used in an alternative analysis that considered an equivalent R -value, R_{eq} , back-calculated from the estimated PGA at the site, with the earthquake magnitude, using a suggested relation in Youd et al. (2002). R -values of 16.9 km and 4 km were used for the September 2010 (M_w 7.1) and February 2011 (M_w 6.2) events, respectively, with the computed values of R_{eq} being 15.5 km and 1 km, respectively.

4.2 Results

The predicted spreading displacements from the two seismic events were summed to compare this cumulative displacement with the field measurement at a given distance from the free-face, L , on an individual transect. The results are presented in Figure 4 for the (a) $R=R$ and (b) $R=R_{eq}$ cases. These comparisons considered field displacements within 10m of the measurement at L to account for variability of measured crack locations over a relatively short distance in the field (represented by the horizontal error bars in the plot). The uncertainty associated with determining F_{15} is represented by the vertical error bars, i.e. computing displacement using the upper and lower bounds of F_{15} and the corresponding $D_{50(15)}$ values. It should be noted that given the form of equation (1), the higher fines content (upper bound of F_{15}) yields a lower displacement, represented by the negative error, and vice versa. The open markers shown in Figure 4 indicate possible restriction of the free-field movement such as field measurements near a bridge abutment.

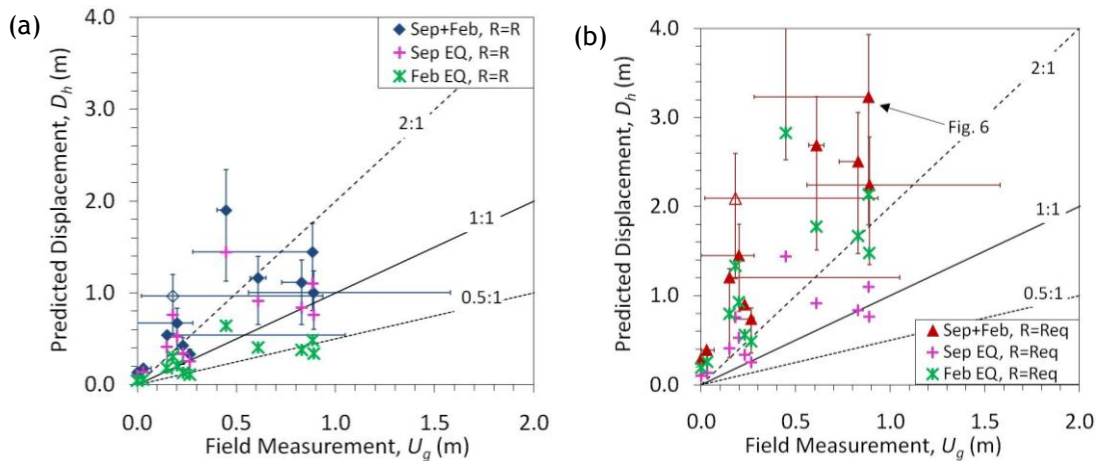


Figure 4. Comparison of field measurements of lateral displacements in the Avon Loop area with empirical predictions from the Youd et al. model using (a) $R=R$ and (b) $R=R_{eq}$

The model shows some agreement (within a factor of two) with the observed displacements at about half of the locations considering the analysis using $R=R$ (actual site-to-source distance) and generally over-predicts the remaining locations (Figure 4(a)). The case considering $R=R_{eq}$ (back-calculated using recorded PGA) showed over-prediction by more than two times at nearly all locations. In addition to the direct comparison, Figure 5 also shows the effects of earthquake magnitude, M_w , and site-to-source distance, R , on the computed prediction. Holding all other factors constant, Figure 5(a) shows larger predictions for the September event (M_w 7.1) despite the smaller R -value used in the analysis of the February event (M_w 6.2). However, the trend reverses as R changes to the R_{eq} -values used for the predictions shown in Figure 4(b). In addition, comparing the two figures reflects how the magnitude of uncertainty associated with F_{15} (vertical error bars) increases by the same factor that the mean displacement increases when decreasing R to R_{eq} , creating a larger variability in the predictions for a given location; i.e. as the predicted mean displacement increases, so does the influence of uncertainty.

4.3 Uncertainties in model application

There are several sources of uncertainty that may attribute to the variation between predicted values and field measurements shown in Figure 4 which include:

- Scatter in the empirical relationships between I_c - FC and FC - D_{50} used to convert CPT data into the geotechnical parameters, F_{15} and $D_{50(15)}$, required for the model and the associated limitations discussed previously.
- Limitations in field measurements of spreading, such as cracks repaired before the time of the investigation, lateral extension of the ground not propagating as measurable cracking, and obstacles in the field hindering continuation of the transect.
- Application of $R_{eq}=1km$ for the February event. The model recommends a minimum R -value of 0.5 km; the application of $R_{eq}=1km$ causes a significant increase (and over-prediction) in all displacements that may be attributed to approaching this limit.
- Uncertainties in groundwater levels that may affect the value of T_{15} .
- Variability in site conditions from the point of exploration (the analysis considered CPTs up to 50m away from transects where spreading displacements were measured).

5 SENSITIVITY ANALYSIS

On account of the bias in the model towards over-prediction of lateral spreading displacements at the site, a sensitivity analysis was performed in order to assess whether this bias can be attributed to uncertainties in the model input. A specific measurement from transect 'T6' was selected for the analysis (location 'A' in Fig. 1). The field measurement of lateral displacement at this location was ~ 0.9 m, with a model prediction of ~ 3.2 m (using R_{eq} , i.e. back-calculated from recorded PGA). The uncertainty ranges for the parameters investigated are based on

changes in channel heights across the site (changing W from 13% to a maximum of 20% as limited by the model recommendations); changes in groundwater levels of ± 1 m (causing a change in T_{15} of $\sim \pm 1$ m); upper and lower bounds of F_{15} (\pm one sigma in Fig. 2) and corresponding $D_{50(15)}$; and the actual site-to-source distance, R .

The sensitivity of predicted displacements was initially assessed by varying a single parameter over its range of values while holding the remaining parameters constant (at the original input value). The results are provided in Figure 5(a) with respect to the predicted and observed displacements. The Youd et al. model exhibits a high sensitivity to all parameters for the uncertainty ranges considered. The form of equation (1) indicates that an increase in F_{15} and an increase in $D_{50(15)}$ will yield a lower displacement; however, Figure 3(b) shows that a higher F_{15} value is typically correlated with a lower $D_{50(15)}$ and the analysis considers these two parameters as coupled. When F_{15} is increased to 35% and the corresponding $D_{50(15)}$ is decreased 0.13mm, the higher F_{15} value dominates the computed displacement and yields a lower prediction. Using $R=R$ (PGA unknown) for the site-to-source distance resulted in a much closer prediction to the observed, indicating the initial analysis considering $R=R$ may be more applicable at the site (rather than the $R=R_{eq}$ analysis), this is also shown in Figure 4(a) with $R=R$ predictions being closer to that observed.

Figure 5(a) illustrated that the model is very sensitive to the input parameters, especially F_{15} and $D_{50(15)}$. A second analysis was performed to determine whether this prediction variation is due to the actual model sensitivity or due to the uncertainty associated in determining the parameters themselves. Each input parameter was individually varied by $\pm 10\%$ and the resulting displacement is shown in Figure 5(b). Figure 5(b) shows that in general, a 10% change in input parameters results in a less than 10% change in predicted displacement. This variation is constant for all cases because of the model functional form. However, while some parameters may be estimated to within 10% at a given location, the grain size characteristics, FC and D_{50} , are typically highly variable within the soil profile and often fluctuate significantly more than 10%. Thus, the sensitivity of the input parameter values, F_{15} and $D_{50(15)}$, in predicting spreading displacements clearly creates difficulty in producing accurate and precise model predictions.

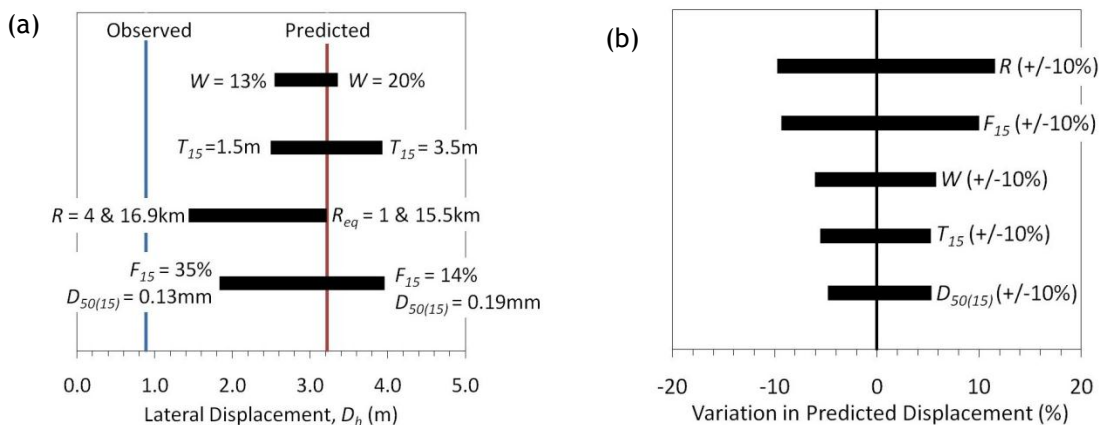


Figure 5. Sensitivity analysis of Youd et al. model relative to (a) parameter uncertainties at location ‘A’ and (b) 10% change in input parameters

6 CONCLUSIONS

Lateral spreading displacement measurements from the Christchurch earthquakes were compared to the empirical model of Youd et al. (2002). Due to the limited availability of borehole and SPT data in proximity to the surveyed locations, the geotechnical parameters (specifically F_{15} and $D_{50(15)}$) were derived from CPT data. The results of the comparison between the Youd et al. model and the observed field data in Christchurch show the analysis considering the actual site-to-source distance, R , to be generally more consistent with the field observations at about half of the locations. In contrast, use of the correlated source-to-site

distance based on the observed PGA, R_{eq} , lead to significant over-prediction of the lateral spreading displacements.

A sensitivity analysis indicates that the model is highly sensitive to all input parameters. The strong influences of F_{15} and $D_{50(15)}$ on the predictions indicate that the uncertainties associated with the derived correlations may be too significant for accurate application of the model. In addition, FC and D_{50} are typically highly variable within the soil profile. These parameters' high degree of sensitivity may be a reflection of the pure empirical and statistical nature of the model's derivation. Future work includes further comparisons with the Youd model and others, with an aim to achieve a more accurate method of lateral spreading predictions in Christchurch.

7 ACKNOWLEDGEMENTS

The authors would like to acknowledge the New Zealand Earthquake Commission (EQC) for their continued financial support for this research.

REFERENCES

- Bradley, B.A., and Hughes, M. (2012) Conditional Peak Ground Accelerations in the Canterbury Earthquakes for Conventional Liquefaction Assessment. *Technical Report for the Ministry of Business, Innovation and Employment*.
- Canterbury Earthquake Recovery Authority (2012) *Geotechnical database for Canterbury earthquake sequence*.
<https://canterburygeotechnicaldatabase.projectorbit.com>.
- Cubrinovski, M., Rees, S. and Bowman, E. (2010). Effects of Non-plastic Fines on Liquefaction Resistance of Sandy Soils. *Earthquake Engineering in Europe*. Garevski, M. and Ansal, A., Springer Netherlands. 17: 125-144.
- Cubrinovski, M., Robinson, K., Taylor, M., Hughes, M. and Orense, R. (2012) Lateral spreading and its impacts in urban areas in the 2010-2011 Christchurch earthquakes. *Special Issue on Canterbury Earthquakes, New Zealand Journal of Geology and Geophysics*, 55(4), 255-269.
- Chu, D.B., Stewart, J.P., Youd, T.L., and Chu, B. (2006) Liquefaction-induced lateral spreading in near-fault regions during the 1999 Chi-Chi, Taiwan earthquake. *Journal of Geotechnical and Geoenvironmental Engineering*, 132(12), 1549-1565.
- Jefferies, M.G. and Davies, M.P. (1993) Use of CPTu to Estimate Equivalent SPT N60. *Geotechnical Testing Journal*, 16: 458.
- Robinson, K., Cubrinovski, M., Kailey, P., and Orense, R. (2011) Field Measurements of lateral spreading following the 2010 Darfield earthquake. *Proceedings of the 9th Pacific Conference on Earthquake Engineering, Auckland, New Zealand*.
- Robinson, K., Cubrinovski, M. and Bradley, B.A. (2012) Lateral Spreading Measurements from the 2010 Darfield and 2011 Christchurch Earthquakes. *Proceedings of the Australia New Zealand Conference on Geomechanics (ANZ)*. Melbourne, Australia: 7.
- Robertson, P.K. and C.E. Wride (1998) Evaluating cyclic liquefaction potential using the cone penetration test. *Canadian Geotechnical Journal*, 35(3): 442-459.
- Youd, T.L., Idriss, I.M., Andrus, R.D., Arango, I., Castro, G., Christian, J.T., Dobry, R., Liam Finn, W.D., Harder L.F., Jr., Hynes, M.E., Ishihara, K., Koester, J.P., Liao, S.S.C., Marcuson Iii, W.F., Martin, G.R., Mitchell, J.K., Moriwaki, Y., Power, M.S., Robertson, P.K., Seed, R.B., and Stokoe Ii, K.H. (2001) Liquefaction resistance of soils: Summary report from the 1996 NCEER and 1998 NCEER/NSF workshops on evaluation of liquefaction resistance of soils. *Journal of Geotechnical and Geoenvironmental Engineering*, 127(10), 817-833.
- Youd, T.L., Hansen, C.M., and Bartlett, S.F. (2002) Revised multilinear regression equations for prediction of lateral spread displacement. *Journal of Geotechnical and Geoenvironmental Engineering*, 128(12), 1007-1017.